Received: 1 October 2023 | Revised: 2 December 2023 | Accepted: 23 December 2023

DOI: 10.1002/cjce.25189

RESEARCH ARTICLE

THE CANADIAN JOURNAL OF CHEMICAL ENGINEERING

# Combination of population balance equation and multi-layer capacitor theory for modelling of an industrial Dual Polarity® electrostatic treater

**Navid Akbarian Kakhki** | **Mohammad Shooshtari** | **Mehdi Karimi**

Faculty of Engineering, Chemical Engineering Department, Ferdowsi University of Mashhad, Mashhad, Iran

**Correspondence**
Mehdi Karimi, Ferdowsi University of Mashhad, Faculty of Engineering, Chemical Engineering Department, Mashhad, Iran
Email: mehdikarimi@um.ac.ir

**Abstract**

In the present study, an analytical model is developed to investigate the dehydration efficiency of a NATCO Dual Polarity® electrostatic treater at steady state conditions using population balance equations (PBE). To investigate the effect of frequency on dehydration performance and electric field strength between electrodes, a detailed electrical model is considered. In the developed electrical model, electrodes are virtualized as simple ideal capacitors, with emulsion acting as dielectric. Proving the model's accuracy, gathered industrial data were compared with simulation results. In addition, current frequency as the main electrical parameter besides power supply electrical potential was proved to be effective on the strength of the applied electric field, the electrical potential profile on electrodes, and the outlet water cut in the treated crude oil. The results indicated that increasing the current frequency from 50 to 500 Hz, by enhancing direct current field strength, reduces the water cut by 0.03%. Although high temperatures and frequencies increase the electrical conductivity of the emulsion, electrical power lost during the disconnection of the power supply on electrodes will be retrieved by increasing frequency. Finally, the performance of different electric fields on crude oil dehydration was compared.

**KEYWORDS**

Dual Polarity®, electrostatic treater, high frequency, multi-layer capacitor, population balance, W/O emulsion

## 1 | INTRODUCTION

The most important impurity in crude oil extracted from oil wells is saltwater. Among the problems that this impurity creates for the industry, we can mention equipment corrosion, pressure drop in pipelines, and reduction of catalyst activity. Separation systems were developed to decrease saltwater in crude oil, reaching commercial specifications. Gravitational and centrifugal settling, thermal treatment, and chemical and electrical methods are known dehydration methods to separate salty water from crude oil.[1–3] Currently, to achieve maximum efficiency, the integration of chemical, thermal, and electrical methods is used in desalting units. The original purpose of applying an electric field is to increase the rate of collision and, as a result, the integration of dispersed water droplets by exerting electrical forces depending on the type of field.[4] Eow and Ghadiri[5] reviewed the fundamentals of the coalescence of droplets comprehensively. The applied electric field can be classified according to the type of current into three categories, including alternating current (AC), direct current (DC), and the combination of

  

alternating and direct currents (AC/DC).[6–8] The dipolar attraction, electrophoresis, and dielectrophoresis are the main electrical forces that affect the electrostatic dehydration. Dipolar attraction is the electrostatic force between oppositely charged particles and is categorized in the short-range forces group. Electrophoresis force is the electrical attraction inside a uniform electric field. Droplets move along the direction of the field due to the electrophoresis force between drops and electrodes. Dielectrophoresis is the force implemented on polarized droplets inside a non-uniform electric field. In W/O emulsions, droplet coalescence occurs when there is enough energy to overcome coalescence obstacles such as film formed on the surface of the droplets, electrical double-layer effects, fines dispersed around the water droplets, and interfacial tension. AC-type crude oil dehydrator is the oldest technology in crude oil treatment. In this technology, the electrical field between electrodes is generated by a high-voltage power supply at a common urban power frequency. The applied field on the crude oil emulsion accelerates droplet collision by creating an attraction force between oppositely charged particles. AC desalters are quite effective for bulk water removal since applied forces are considered in short-range group. DC fields provide superior coalescence due to the electrophoretic force between droplets and electrodes. However, DC-type desalters suffer from electrocorrosion and electrical short-circuit in the power supply, in the case of water-rich emulsion treatment due to droplet chain formation between electrodes. In 1972, Dual Polarity® technology was proposed by NATCO company with a combination of both AC and DC electric fields. In the presented technology, the crude oil emulsion is initially subjected to a weak AC field to remove large water droplets followed by a strong DC field to achieve the required dehydration target. This technology can separate very small droplets that are not usually separated by AC-field. Reducing the consumption of electrical energy is also considered one of the advantages of this system since it consumes about 40% less power than the AC field. Due to the increase in the efficiency of dewatering and desalination in the AC/DC electric field, the dimensions of the coalescer tank and the amount of demulsifier injection are reduced compared to the AC electric field.

Many works of research have been conducted on the separation of water from crude oil, especially using the electrical method. Using molecular dynamics simulation, Chen et al.[9] investigated dehydration of crude oil in AC electric field. The results indicated that implemented dipole forces increases the droplet collision rate. Shooshtari et al.[10] modelled with good accuracy an industrial electrostatic coalescer with an alternating electric field using the population balance equation (PBE). The results showed that by reducing crude oil American Petroleum Institute (API) gravity from 33 to 30, the efficiency of dehydration decreases by 2.88%. Peng et al.[11] simulated the simultaneous effect of heating, electric, and centrifugation fields on crude oil dehydration. The results showed that the combination of these three factors increases the rate of dehydration. The proposed model predicted the efficiency of the process well. Also, the simulation results represented that the efficiency of the process improves with increasing voltage and temperature. Bailes and Larkai[12,13] improved the collision of water drops by the selection of the appropriate electrical parameters for a pulsed DC field and electrode insulation experimentally. Finally, it was determined that the system should be modelled based on a two-layer capacitor. The modelling results indicated the optimal frequency of the DC electric field based on the electrical properties and the thickness of both the electrode coating and the emulsion. Bailes[14] used a resistor–capacitor model to survey the effect of frequency and type of electrode's insulation on voltage decay and desalting efficiency based on an electric circuit model. Barega et al.[15] used the population balance model to investigate the effect of a square wave frequency on the coalescence rate of toluene in water emulsion. Electrodes were covered by two insulation layers and the results were validated by measuring the mean square diameter of droplets.

In the present paper, the dehydration efficiency of the Dual Polarity® electrostatic treater was studied by combining the electrical circuit model and one-dimensional steady-state PBE. In the second part, the mathematical equations for modelling the electrostatic treater, the mixing valve, and the considered assumptions are mentioned. In the third part, the numerical method to solve the PBE is presented. In the fourth section, the results of the modelling and operational analysis of the dual polarity electrostatic desalination process are discussed.

## 2 | PROCESS MODELLING

Various methods such as Eulerian multi-fluid, Euler–Lagrange, and PBE have been introduced to predict the dispersion of droplets in the continuous phase.[16–19] The PBE as an accurate method is about the balance of the mean number density and considers the destruction and coalescence of emulsion droplets in terms of physical parameters. The number density function is related to the droplet properties, residence time, and physical space.[20] The PBE for liquid–liquid emulsion systems is based on changes in particle size distribution due to coalescence and breakage terms. In this paper, the Dual Polarity® electrostatic treater and mixing valve are modelled at steady-state conditions.

## 2.1 | Electrical circuit model

Figure 1 displays a diagram of the Dual Polarity® system schematically. In the present design, vertical plates which are powered alternately with positive and negative charges are installed along the length of the treater. The power supply and electric circuit are designed to provide positive and negative charges on plates in opposite half-periods, and as a result, the voltage gradient on the droplets is doubled.

Figure 2 shows the developed electrical circuit model for the Dual Polarity® technology. To generate the desired field among electrodes, high voltage AC sinusoidal wave passes through rectifiers which have been designed in the opposite direction to separate positive and negative pulses and create a DC electric field between electrodes during all periods. In other words, during the first half of each period when the source electrical potential has higher potential against the earth, the first rectifier is open and the second one is closed, providing stable positive potential

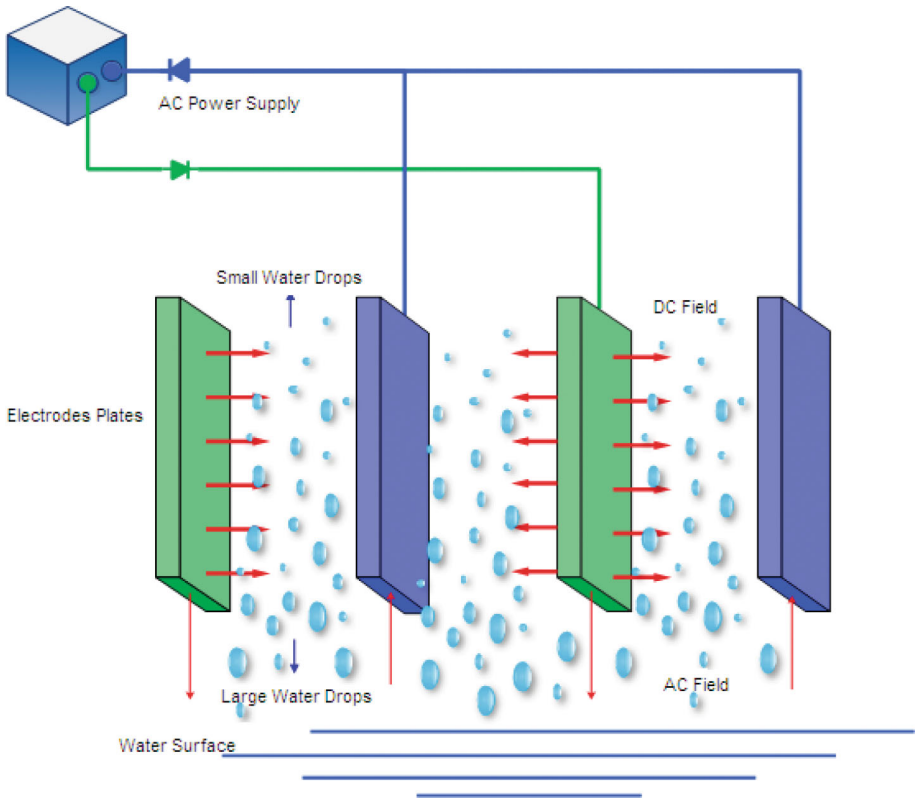


**FIGURE 1** Electrode arrangement in Dual Polarity® electrostatic treater. AC, alternating current; DC, direct current.

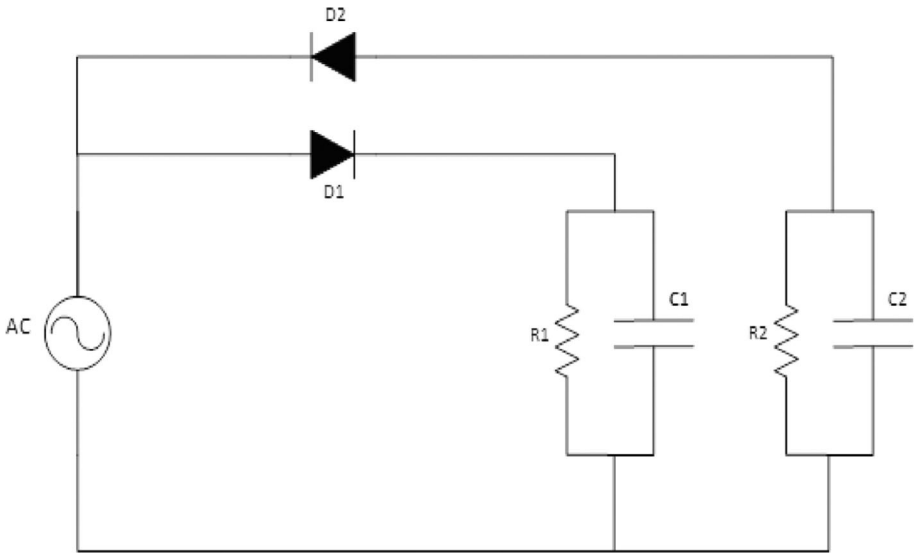


**FIGURE 2** The considered electrical circuit of the system. AC, alternating current.

on the first group of electrodes. In the second half of the period, by reversing the rectifier on–off position, the negative pulses pass, and the next set of electrodes are charged with the negative potential.

During the rectifier off time, the virtual capacitor releases its electrical energy to establish the internal current network in the interior loops of the circuit. This process leads to a loss of electrical charges on the surface of electrodes, which decreases the electrical potential exponentially. Considering a normal sinusoidal waveform, electrical potential variation with time on each electrode in the DC field can be defined as follows:

$$V = \begin{cases} V_{\max}\sin(\omega t) & t < t_1 \\ V_{\max}\sin(\omega t_1)\mathrm{e}^{\frac{-(t-t_1)}{CR}} & t_1 < t < t_2 \end{cases}, \tag{1}$$

$$t_1 = \frac{\pi - \psi}{\omega}, \tag{2}$$

$$\psi = \tan^{-1}(\omega cR), \tag{3}$$

where $t_1$ and $t_2$ are off-time and on-time of power supply, respectively. The rate of electrical potential decay during the off-time period is related to the capacity and resistance of the hypothetical capacitor directly and can be calculated with Equations (4) and (5), respectively.

$$C = \frac{\varepsilon_0 \varepsilon_r A}{d}, \tag{4}$$

$$R = \frac{d}{\kappa \cdot A}, \tag{5}$$

In the above correlations, $d$, $A$, $C$, and $R$ are the distance between plates, area of each plate, capacitance, and resistance, respectively. $\varepsilon_0$, $\varepsilon_r$, and $\kappa$ are vacuum permittivity, dielectric constant, and emulsion conductivity, respectively. Therefore, having the electric potential behaviour in the positive and negative plates, at a certain frequency, the potential difference between the plates can be calculated. Since the distance between the plates is small in comparison with the dimensions of the plates, the electric field is assumed to be uniform and the electric field intensity will be calculated by dividing the equivalent potential difference by the distance between these plates. Hanai et al.[21] studied dielectric properties of O/W and W/O and showed that there is an exception in the dielectric behaviour of water in oil system due to the dielectric dispersion phenomenon related to interfacial polarization. The complex formats of Debye correlation for dielectric constant and conductivity of emulsion are as follows:

$$\varepsilon' - j\varepsilon'' = \varepsilon_h + \frac{\varepsilon_l - \varepsilon_h}{1 + \left(\frac{jf}{f_0}\right)^{1-\alpha}}, \tag{6}$$

$$\kappa' - j\kappa'' = \kappa_h + \frac{\kappa_l - \kappa_h}{1 + \left(\frac{jf}{f_0}\right)^{1-\alpha}}. \tag{7}$$

Hanai et al.[21] introduced correlations for high- and low-frequency dielectric constant and conductivity of crude oil emulsion.

$$\frac{\varepsilon_p - \varepsilon_h}{\varepsilon_p - \varepsilon_m}\left(\frac{\varepsilon_m}{\varepsilon_h}\right)^{1/3} = 1 - \phi, \tag{8}$$

$$\varepsilon_h = \frac{\varepsilon_m}{(1-\phi)^3}, \tag{9}$$

$$\frac{\kappa_l}{\kappa_m} = \frac{1}{(1-\phi)^3}, \tag{10}$$

$$\frac{\kappa_h}{\kappa_h} = \frac{3\varepsilon_h(\varepsilon_h - \varepsilon_m)}{(2\varepsilon_h + \varepsilon_p)(\varepsilon_p - \varepsilon_m)}. \tag{11}$$

Salt concentration and temperature impact on the relative permittivity of aqueous solutions is considered by Zuber et al.[22]

$$\varepsilon_p = \frac{\varepsilon_s}{1 + \sum_{i}^{\text{ion}} \gamma_i x_i}, \tag{12}$$

$$\varepsilon_s = d_1 + \frac{d_2}{T} + d_3 T + d_4 T^2 + d_5 T^3. \tag{13}$$

There are some correlations to determine the conductivity of sodium chloride aqueous solution in terms of salt concentration in the literature. Typically, the conductivity of an aqueous solution increases with temperature and salt concentration. Temperature compensation is a useful method to consider the temperature effect on the aqueous solution conductivity.

$$\kappa_{25} = \frac{\kappa_T - \kappa_W}{1 + 0.02(T - 25)} + 0.0545. \tag{14}$$

## 2.2 | Mathematical model

In the present study, the mixing valve and Dual Polarity® electrostatic treater are modelled according to PBE. The considered assumptions are presented below:

- No destruction of droplets due to applied electric fields in the treater
- One-dimensional movement of emulsion
- Steady-state condition

Considering the above assumptions, the steady-state one-dimensional PBE can be written as follows:

$$u_k \frac{dN(l_k)}{dy} = S_k, \tag{15}$$

where $N$, $u_k$, and $S_k$ are the mean number density function, the relative velocity of water droplets, and the rate of death and birth of droplets with class size $k$, respectively.

$$S_k = B_k^c - D_k^c + B_k^b - D_k^b, \tag{16}$$

$$B_k^c = \frac{1}{2}\int_0^{l_k} \beta(l_i, l_j) \cdot N(l_i) \cdot N(l_j) dl, \tag{17}$$

$$D_k^c = N(l_k) \cdot \int_0^{\infty} \beta(l_k, l_j) \cdot N(l_j) dl, \tag{18}$$

$$B_k^b = \int_l^{\infty} g(l) \cdot P(l|l_i) \cdot N(l) dl, \tag{19}$$

$$D_k^b = g(l_k) \cdot N(l_k). \tag{20}$$

Correlations (17)–(20) show the creation of larger drops due to the coalescence of smaller ones, the death of a drop due to the coalescence with another droplet, the birth of a droplet due to the breakup of a larger droplet, and the death of a droplet due to a breakup, respectively.

MATLAB software was used to calculate characteristics and solve developed equations in main code which was accompanied by auxiliary functions. The dual polarity treater's internal space was discretized into small elements and for each element developed equations were solved to get to a new droplet size distribution. Inside each element, considering water cut, electrical characteristics of emulsion were calculated with auxiliary functions and used for electrostatic field strength estimation which is critical for the calculation of collision frequency of droplets inside the element. By solving all equations, a new droplet size distribution is used to modify old data until convergence is reached.

### 2.2.1 | Mixing valve

Although severe turbulence inside the mixing valve provides a suitable situation for mixing fresh water and crude oil, leading to a reduction of salt concentration, it causes undesirable destruction of large droplets. Droplet breakage in this system occurs due to surface and viscous forces. Considering the effect of both forces, Alopaeus et al[23] proposed the following function to determine the droplet breakage rate:

$$g(d) = C_1 \xi^{1/3} erfc\left(\sqrt{\frac{C_2\sigma}{\rho_c d^{5/3}\xi^{2/3}} + \frac{C_3\mu_d}{\sqrt{\rho_c\rho_d} d^{4/3}\xi^{1/3}}}\right). \tag{21}$$

In Equation (21), $\xi_c$ is the rate of energy dissipation, respectively, and is determined through the following equation:

$$\xi_c = \frac{\Delta P}{t_{res}\rho_c}. \tag{22}$$

It is worth noting that for a capillary number less than the critical value, the droplet will not break and, as a result, the droplet breakage frequency will be zero. The breaking of drops in the mixing valve is not binary, so the following function is applied to predict the probability of a smaller droplet's formation with a volume of $V$ due to the disintegration of a larger droplet with a volume of $V_0$[24]:

$$f(V, V_0) = m(m-1)\left(1 - \frac{V}{V_0}\right)^{m-2}. \tag{23}$$

Turbulence forces improve the collision process of droplets besides the breakage phenomenon. Therefore, the following equation is used to determine the droplet coalescence rate in the mixing valve[25]:

$$\beta(l_i, l_j) = C_4 \cdot \frac{\xi^{1/3}}{1+\phi}(l_i + l_j)^2\left(l_i^{2/3} + l_j^{2/3}\right)^{1/2} \times e(l_i, l_j), \tag{24}$$

$$e(l_i, l_j) = \exp\left(-\frac{0.71\mu_w\left(h_i^{1/2} - h_f^{1/2}\right)}{\rho_o\xi^{1/3} l_i^{1/2} l_j^{1/2}(l_i + l_j)^{5/6}}\right), \tag{25}$$

where $h_i$ and $h_f$ are the thickness of the initial film and the critical breaking thickness of the droplets, respectively.

### 2.2.2 | Dual Polarity® electrostatic treater

In the modelling section, the desalting drum is discretized and population balance is developed for each section. In the presence of an electric field due to the electrical forces, the collision rate between fine water

droplets increases, droplets coalesce together, and larger droplets are formed. The larger droplets produced enter the lower element after settling. Finer droplets are taken by the crude oil flow toward top elements. As mentioned earlier, droplets do not break up in a treater, therefore, the death or birth of droplets, which causes the number of droplets to change, depends only on the process of merging droplets. The function $\beta$ is expressed as follows.

$$\beta(l_i,l_j)=\frac{K\pi}{4}(l_i+l_j)^2 V_{ij}\, e(l_i,l_j), \tag{26}$$

$$V_{ij}=\frac{(\dot{\mu}+1)|\rho_c-\rho_d|l_i^2\left(1-\lambda_{i,j}^2\right)g}{6(3\dot{\mu}+2)\mu_c}, \tag{27}$$

$$\lambda_{i,j}=\frac{l_j}{l_i}. \tag{28}$$

Manga and Stone introduced a correlation for collision efficiency in non-electric field systems.[26] In this correlation, $B_i$ is the Bond number and is defined as the ratio of internal forces to the surface tension between two immiscible liquids.[26]

$$e_{i,j}=0.3\left(\frac{l_j}{l_i}\right)^{0.5}+0.5.B_i\left(\frac{l_j}{l_i}\right)^6, \tag{29}$$

$$B_i=\frac{|\rho_c-\rho_d|gl_i^2}{4\sigma}. \tag{30}$$

Collision efficiency in electric field was introduced by Zhang et al.[27]

$$e_{ij}=0.45Q_E(l_i,l_j)^{-0.55}\, l_i\geq l_j, \tag{31}$$

$$Q_E(l_i,l_j)=\frac{2(\mu_d-\mu_c)\lambda_{i,j}(1-\lambda_{i,j})gl_i}{3E^2\epsilon(1+\lambda_{i,j})^2}, \tag{32}$$

## 3 | SOLUTION METHOD

Several numerical methods have been introduced to solve the PBEs, including Monte Carlo[28] weighted residuals,[29] the method of classes,[30] and conventional and modified moments methods.[31] In the present article, the method of classes is chosen for solving PBEs in steady-state conditions due to its simplicity and accuracy, besides its ability to apply droplet size distribution data obtained by laboratory measurement instruments such as focused beam reflectance measurement (FBRM).

In this work, the method proposed by Lister et al.[32] is used to solve the PBE with the classes method. Equations (33) and (34) respectively show the discrete form of PBE for the mixing valve and Dual Polarity® treater:

$$\begin{aligned}u_k\frac{\Delta N(l_k)}{\Delta y}=&\sum_{i=1}^{N}\sum_{j=1}^{N}\beta(l_i,l_j)\cdot N(l_i).N(l_j)\cdot\delta_{i,j}\cdot\omega_{i,j}\\&-\sum_{j=1}^{N}\beta(l_k,l_j)\cdot N(l_k)\cdot N(l_j)\\&+\sum_{i=k+1}^{N}N(l_i)\cdot g(l_i)\cdot P(l_i|l_k)-g(l_k)\cdot N(l_k),\end{aligned} \tag{33}$$

$$\begin{aligned}u_k\frac{\Delta N(l_k)}{\Delta y}=&\sum_{i=1}^{N}\sum_{j=1}^{N}\beta(l_i,l_j)\cdot N(l_i)\cdot N(l_j)\cdot\delta_{i,j}\cdot\omega_{i,j}\\&-\sum_{j=1}^{N}\beta(l_k,l_j)\cdot N(l_k)\cdot N(l_j).\end{aligned} \tag{34}$$

The parameters $\omega$ and $\delta$ are determined as follows:

$$\omega=\begin{cases}1 & for\ V_k<V_c<V_{k+1}\\ 0 & \text{elsewhere}\end{cases}, \tag{35}$$

$V_c$ is the droplet volume resulting from the coalescence of droplets $i$ and $j$, and is defined by using the following equation:

$$V_c=\left[\delta_{i,j}V_k+(1+\delta_{i,j})V_{k+1}\right], \tag{36}$$

where:

$$\delta_{i,j}=\frac{V_c-V_{k+1}}{V_k-V_{k+1}}. \tag{37}$$

## 4 | RESULT AND DISCUSSION

In this part, simulation results of the mixing valve and Dual Polarity® electrostatic treater are presented at steady-state conditions. Applying the method of classes to solve developed equations as a reference for the prediction of water cut and pounds per thousand barrels (PTB) in treated oil, 110 homogeneous size classes ranging from 0.05 to 1200 μm were considered. In general, the efficiency of a desalting unit is expressed in PTB, which is defined as pounds of salt in the treated oil per thousand barrels. Proving the validity and accuracy of the proposed

model and assumptions, desalting and dehydration efficiencies in accordance with simulation outputs are compared with the plant data of an industrial crude oil desalting unit. Tables 1 and 2 show the feed specification and characteristics of the considered electrostatic treater and electrical properties of the emulsion, respectively. Comparison between simulation results and gathered plant data are presented in Table 3. It is clear that predicted dewatering and desalination efficiencies are close to the industrial data.

**TABLE 1** Operating conditions of considered industrial electrostatic treater.

| Property | Value |
|---|---|
| Feed | |
| Crude oil rate (bbl · day$^{-1}$) | 60,000 |
| Crude oil temperature (°C) | 51 |
| API | 33.04 |
| Water cut (%) | 10 |
| Crude oil salt content (PTB) | 81.69 |
| Fresh water | |
| Flow rate | 5% of crude oil rate |
| Temperature (°C) | 50 |
| Mixing valve | |
| Pressure drop (psi) | 25 |
| Mixing efficiency (%) | 100 |
| Desalting drum | |
| Length (m) | 13.72 |
| Diameter (m) | 3.05 |
| Electrodes length (m) | 0.3 |

Abbreviations: API, American Petroleum Institute; PTB, pounds per thousand barrels.

**TABLE 2** Electrical properties of emulsion phases at the standard condition and pure form.

| | Oil phase | Water phase |
|---|---|---|
| Electrical conductivity (S · m$^{-1}$) | $3.83 \times 10^{-8}$ | $4.26 \times 10^{-6}$ |
| Dielectric constant | 2.5 | 78.2 |

**TABLE 3** Comparison between simulation results and industrial data at steady state conditions.

| | Modelling result | Industrial data |
|---|---|---|
| Dehydration efficiency | 99.23 | 99.16 |
| PTB | 3.54 | 3.78 |

Abbreviation: PTB, pounds per thousand barrels.

## 4.1 | Mixing valve

The size distribution of water drops at the outlet of the mixing valve is shown in Figure 3. The purpose of using a mixing valve is to provide a sufficient mixing between fresh water and dispersed saline droplets. Indeed, dilution reduces the concentration of dissolved salt in the outgoing crude. Generally, the mixing valve provides a suitable shear force in the range of 10–25 psi of differential pressure. As large droplets break up into small ones, the peak of the droplet size distribution shifts from 86 μm in the inlet flow to 64 μm in the outlet flow.

## 4.2 | Dual Polarity® electrostatic treater

In the present study, the Dual Polarity® electrostatic treater is divided into three sections according to the treater geometry and type of electric field. Initially, distributed oil flow moves upward and at non-electric field area and large droplets move to lower layers due to gravitational force. In the second section, between the water–oil interface and electrodes, there is a weak dipolar–dipolar attraction force between the droplets due to the AC electric field. The electrical power source connected to the electrode plates provides a sinusoidal wave at 50 Hz frequency and 20 kV peak voltage. In the last part of the separation, in the presence of the DC electric field between the electrode plates, the droplet collision rate increases and therefore larger droplets are formed. Figure 4 shows the size distribution of water drops along the electrostatic drum. Crude oil emulsion enters the first section and

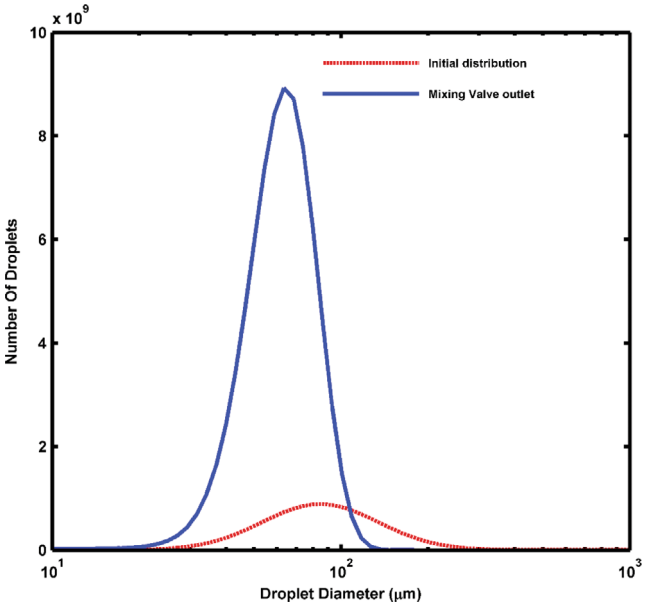


**FIGURE 3** Droplets size distribution in the mixing valve.

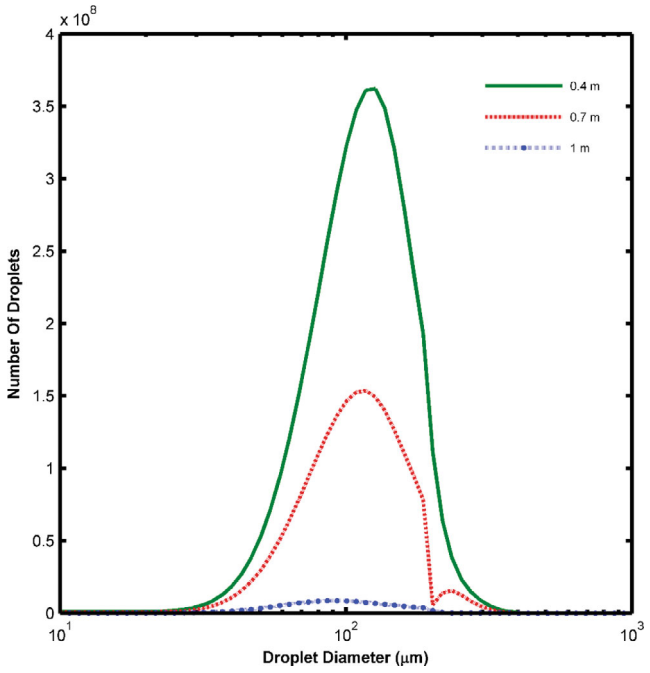


FIGURE 4 Water droplet size distribution in the different sections of the electrostatic treater.

moves upwards. In this part, the coarse droplets are deposited and the fine droplets are carried upwards by the crude oil and enter the second part. In general, water drops with a diameter larger than the Stokes diameter settle. It appears that as the crude oil flows to the top of the electrostatic drum, the small droplets coalesce to form larger droplets that have the ability to settle, thus a minimum droplet size distribution appears at the top of the drum. In addition, the rate of droplet coalescence increases in the DC field section due to the electrophoretic forces acting on the droplets.

### 4.2.1 | Effect of frequency on electric potential

The electrical properties of crude oil have an important effect on the strength of the electrostatic field. In the case of high-conductivity crude oil refining, the electrical potential between the electrode plates decreases during the rectifier off-time, resulting in a loss of field strength. Figure 5A shows the electric potential profile in the positive and negative set of electrodes, while the power source applies a sinusoidal wave with 20 kV maximum voltage at 50 Hz. Dielectric properties of emulsion change the charge storage on the electrode plates. However, due to the high conductivity of emulsion, this charge accumulation is not much and results in the faster consumption of stored energy during the rectifier off time. The main procedure to improve the total charge accumulation on

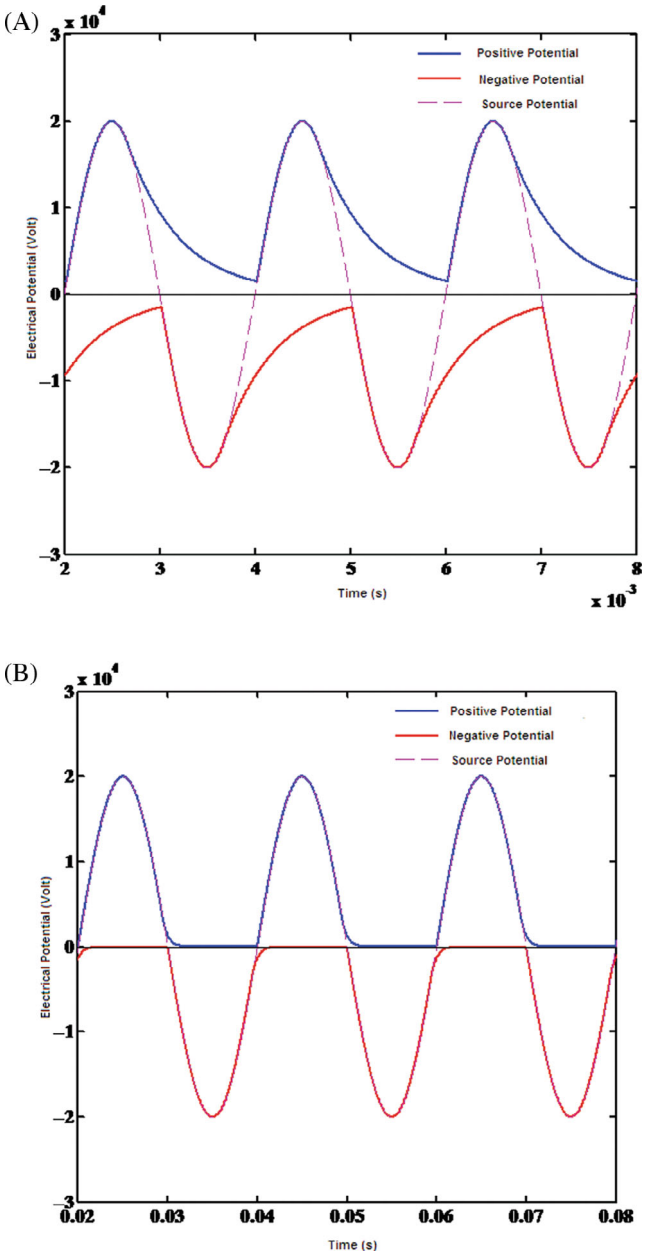


FIGURE 5 Electric potential profile in negative and positive electrodes at (A) 50 Hz and (B) 500 Hz.

the surface of electrode plates is to increase frequency in order to rapid re-charge virtual capacitor and prevent potential decay in off time, which results in a stronger electric field and higher coalescence rate of droplets. This solution is a trial and error method which is done by control operator according to variation of feed and its characteristics. So, providing a solution to predict electric field strength variation according to characteristics of emulsion is valuable. Although increasing frequency improves the conductivity of emulsion by affecting electrochemical characteristics of continuous and dispersed phases, it increases average electrical

**TABLE 4** Effect of current frequency on strength of the electric field, water cut, and dehydration efficiency.

| Frequency (Hz) | DC electric filed strength (kV · m$^{-1}$) | Water cut (%) | Dehydration efficiency (%) |
|---|---|---|---|
| 50 | 108.9 | 0.080 | 99.23 |
| 100 | 110 | 0.079 | 99.24 |
| 200 | 116 | 0.074 | 99.29 |
| 300 | 125 | 0.068 | 99.35 |
| 400 | 135 | 0.062 | 99.41 |
| 500 | 144 | 0.057 | 99.45 |

Abbreviation: DC, direct current.

potential on electrodes overall. It is clear from Figure 5B that increasing frequency from 50 to 500 Hz improved the strength of the applied DC electric field on the emulsion from 108 to 144 kV m.

### 4.2.2 | Effect of frequency on crude oil dehydration and water cut

Table 4 displays the effect of frequency on the water content in the treated crude oil and dehydration efficiency of the Dual Polarity® electrostatic desalting process. It appears that there is a nonlinear relationship between frequency and strength of the applied DC field, so the effect of frequency variation is more significant on the electric field at higher frequencies. The rate of increase in the electric field in the range of 50–100 Hz is about 0.04 kV m$^{-1}$ Hz$^{-1}$ and it increases to 0.06 and 0.093 kV m$^{-1}$ Hz$^{-1}$ in the ranges of 100–200 and 200–300 Hz, respectively. It is clear that the current frequency changing from 50 to 500 Hz declined the remaining water in the outlet flow of crude oil from 0.08% to 0.057%. Since the main aim of the desalting process is to reduce the water cut to below 0.1%, increasing the current frequency can increase the crude oil capacity in the conventional desalting units considering the required criteria for water cut and PTB in the outlet treated crude oil.

Based on the results in Table 4, it can be concluded that the effect of current frequency on the dehydration efficiency and water cut is marginal.

### 4.2.3 | Effect of temperature on crude oil dehydration

Temperature as a mostly known operational variable affects the crude oil dehydration efficiency in two different ways. Increasing temperature influences the physical properties of the continuous phase such as viscosity, density, and surface tension. Decreasing the viscosity of continuous phase enhances the rate of droplets settling significantly according to Stokes' law. It also affects dispersed and

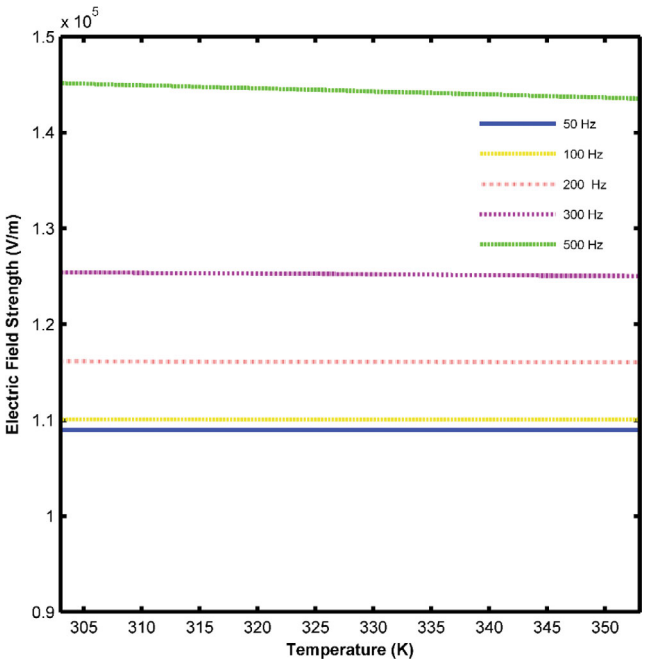


**FIGURE 6** Effect of temperature on the applied electric field on the emulsion.

continuous phase's electrical properties. Rising in temperature increases the electrical conductivity of emulsion and leads to a reduction of electric potential difference between electrode plates. Figure 6 shows the DC electric field strength between electrodes versus temperature at various current frequencies. It appears that although the temperature has an insignificant effect on the electric field intensity at low frequencies, increasing it from 30 to 80°C decreases the field power about 1.6 kV m$^{-1}$. Table 5 presents the electric field intensity and water cut at various temperatures and frequencies.

### 4.2.4 | Effect of different electric fields on crude oil dehydration

In order to investigate the effect of different electric fields on the dehydration of crude oil, the performance of three

| Frequency (Hz) | DC electric field intensity (kV · m$^{-1}$) | | | Water cut (%) | | |
|---|---|---|---|---|---|---|
| | 30°C | 50°C | 80°C | 30°C | 50°C | 80°C |
| 50 | 108.97 | 108.97 | 108.97 | 0.22 | 0.080 | 0.029 |
| 150 | 112.53 | 112.51 | 112.49 | 0.21 | 0.077 | 0.028 |
| 300 | 125.42 | 125.27 | 125.02 | 0.19 | 0.067 | 0.024 |
| 500 | 145.1 | 144.51 | 143.54 | 0.16 | 0.055 | 0.019 |

Abbreviation: DC, direct current.

**TABLE 5** Electric field intensity and water cut at different temperatures and frequencies.

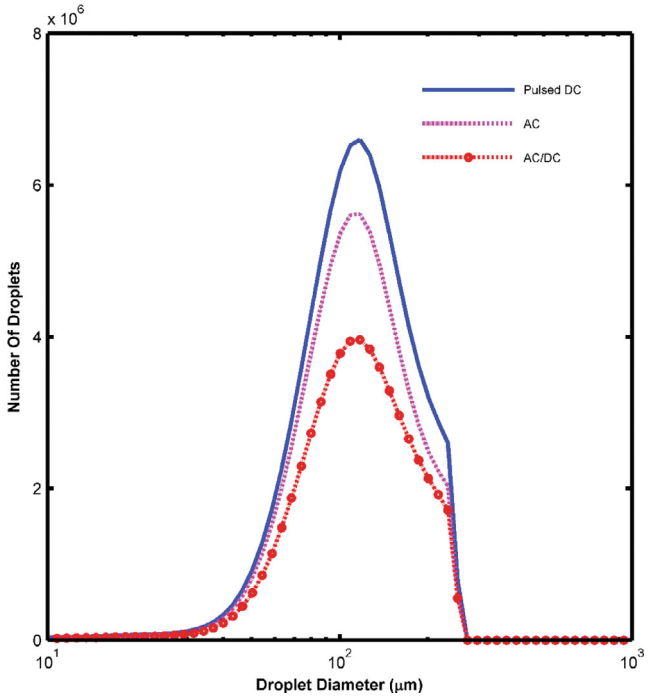


**FIGURE 7** Droplet size distribution at the output of electrostatic treater in different electric fields. AC, alternating current; DC, direct current.

electric fields AC, DC, and AC/DC were compared. Figure 7 illustrates size distribution of the output water droplets at different fields. It is known that the number of water droplets in the output oil in Dual Polarity® field is less compared to AC and DC fields. In the Dual Polarity® system the emulsion first loses a significant part of its water under the influence of a weak AC electric field, and then, under the influence of a strong DC electric field, the remaining fine droplets will be separated. The modelling results showed that for the same inlet size distribution (initial water content 10% and frequency 50 HZ), the efficiency of dewatering in DC, AC, and AC/DC fields is 98.82%, 99.05%, and 99.24%, respectively. Electrical forces are stronger in DC field, but electric potential reduction due to short-circuit and chain formation reduces dehydration efficiency. Therefore, the efficiency of separating water from crude oil in the DC electric field is lower than in the AC electric field.

## 5 | CONCLUSION

In the currentwork, the Dual Polarity® electrostatic treater was modelled by PBE in association with multi-layer capacitor theory. To consider the effect of electrical properties on separation efficiency, internal electrodes and emulsion were hypothesized as an ideal capacitor. The accuracy of the presented model was proved by comparing the output of the model and industrial data. Then, the effect of frequency on electric field, electrical potential between electrodes, and water cut in the treated crude oil was investigated. The simulation results revealed that boosting frequency from 50 to 500 Hz enhances the strength of the DC electric field from 108 to 144 kV · m$^{-1}$, respectively. In addition, it reduced the proportion of water in outlet crude oil from 0.08% to 0.05%. Although the temperature has an insignificant effect on the electric field intensity at low frequencies, operating at high temperature and applying high current frequency on the system increases the electrical conductivity of emulsion and leads to a lower electric potential difference between electrode plates. It was concluded from simulation results that the electrodes play the role of power supply in the system and avoid voltage decay during the power supply off-time. In addition, comparison of the performance of the electrostatic treater in different electric fields showed that the Dual Polarity® technology is more effective than application of AC and DC fields alone.

## NOMENCLATURE

| | |
|---|---|
| $A$ | capacitor plate area (m$^2$) |
| $B$ | birth function |
| $C$ | capacitance (F) |
| $C_1$, $C_2$, $C_3$, $C_4$ | adjustable parameter |
| $D$ | death function |
| $d$ | electrode plate distance (m) |
| $e$ | collision frequency function efficiency |
| $f$ | frequency (Hz) |
| $f_0$ | critical frequency (Hz) |
| $g$ | gravitational constant (m · s$^{-2}$) |
| $K$ | arbitrary constant |
| $l$ | droplet characteristic length (m) |
| $N$ | size distribution function |

| | |
|---|---|
| $P$ | pressure (Pa) |
| $R$ | resistance (Ω) |
| $S$ | accumulation |
| $T$ | temperature (K) |
| $u$ | velocity (m/s) |
| $V_{ij}$ | relative velocity (m/s) |
| $x$ | salt molar concentration (M) |
| $y$ | vertical coordinate |

### Greek symbols

| | |
|---|---|
| $\alpha$ | arbitrary constant |
| $\beta$ | collision coefficient |
| $\gamma$ | ion coefficients |
| $\varepsilon$ | dielectric constant |
| $\kappa$ | conductivity ($S \cdot m^{-1}$) |
| $\lambda$ | relative length |
| $\mu$ | viscosity ($Pa \cdot s$) |
| $\dot{\mu}$ | viscosity ratio |
| $\rho$ | density ($kg \cdot m^{-3}$) |
| $\sigma$ | surface tension ($N \cdot m^{-1}$) |
| $\upsilon$ | kinematic viscosity ($m^2 \cdot s^{-1}$) |
| $\xi$ | rate of energy dissipation ($m^2 \cdot s^{-3}$) |
| $\phi$ | water fraction in emulsion |

### Superscripts

| | |
|---|---|
| c | coalescence |
| $'$ | real part |
| $''$ | imaginary part |

### Subscripts

| | |
|---|---|
| i, j, k | class number index |
| c | continuous |
| d | dispersed phase |
| p | particles |
| m | media |
| r | relative |
| l | low frequency |
| h | high frequency |

## AUTHOR CONTRIBUTIONS

**Navid Akbarian Kakhki:** Conceptualization; investigation; software. **Mohammad Shooshtari:** Software; investigation; conceptualization. **Mehdi Karimi:** Validation; supervision.

## PEER REVIEW

The peer review history for this article is available at https://www.webofscience.com/api/gateway/wos/peer-review/10.1002/cjce.25189.

## DATA AVAILABILITY STATEMENT

The data that support the findings of this study are available from the corresponding author upon reasonable request.

## REFERENCES

[1] M. Fortuny, C. B. Oliveira, R. L. Melo, M. Nele, R. C. Coutinho, A. F. Santos, *Energy Fuels* **2007**, *21*, 1358.
[2] C. Holtze, R. Sivaramakrishnan, M. Antonietti, J. Tsuwi, F. Kremer, K. D. Kramer, *J. Colloid Interface Sci.* **2006**, *302*, 651.
[3] D. Sun, X. Duan, W. Li, D. Zhou, *J. Membr. Sci.* **1998**, *146*, 65.
[4] J. S. Eow, M. Ghadiri, A. O. Sharif, T. J. Williams, *Chem. Eng. J.* **2001**, *84*, 173.
[5] J. S. Eow, M. Ghadiri, *Chem. Eng. J.* **2002**, *85*, 357.
[6] P. J. Bailes, P. D. Dowling, *J. Electrost.* **1985**, *17*, 321.
[7] P. J. Bailes, D. Freestone, G. Sams, *Chem. Eng.* **1997**, *644*, 34.
[8] S. D. Brady, F. M. Seibert, (Goulf Production Co), *USA, US1290369A,* 1919.
[9] T. Chen, R. Mohammed, A. Bailey, P. Luckham, S. Taylor, *Colloids Surf., A* **1994**, *83*, 273.
[10] M. Shooshtari, M. Karimi, M. Panahi, *Sep. Sci. Technol.* **2023**, *58*, 1306.
[11] Y. Peng, B. Yu, X. Zhang, H. Gong, Y. Liu, *Chem. Eng. Process.* **2020**, *148*, 107803.
[12] P. Bailes, S. Larkai, *Trans. Inst. Chem. Eng.* **1981**, *59*, 229.
[13] P. Bailes, S. Larkai, *Trans. Inst. Chem. Eng.* **1982**, *60*, 115.
[14] P. Bailes, *Chem. Eng. Res. Des.* **1995**, *73*, 559.
[15] E. W. Barega, E. Zondervan, A. B. de Haan, *Chem. Eng. Sci.* **2013**, *104*, 727.
[16] F. Azizi, A. Al Taweel, *Chem. Eng. Sci.* **2010**, *65*, 6112.
[17] M. Massot, F. Laurent, D. Kah, S. De Chaisemartin, *SIAM J. Appl. Math.* **2010**, *70*, 3203.
[18] G. H. Yeoh, C. P. Cheung, J. Tu, *Multiphase Flow Analysis Using Population Balance Modeling: Bubbles, Drops and Particles*, Butterworth-Heinemann, Oxford, UK **2013**.
[19] B. Selma, R. Bannari, P. Proulx, *Chem. Eng. Sci.* **2010**, *65*, 1925.
[20] D. Ramkrishna, *Population Balances: Theory and Applications to Particulate Systems in Engineering*, Academic Press, San Diego, CA **2000**.
[21] T. Hanai, N. Koizumi, R. Goto, *Bull. Inst. Chem. Res., Kyoto Univ.* **1962**, *184*, 143.
[22] A. Zuber, L. Cardozo-Filho, V. F. Cabral, R. F. Checoni, M. Castier, *Fluid Phase Equilib.* **2014**, *376*, 116.
[23] V. Alopaeus, J. Koskinen, K. Keskinen, J. Majander, *Chem. Eng. Sci.* **2002**, *57*, 1815.
[24] N. Raikar, S. Bhatia, M. Malone, D. McClements, C. Almeida-Rivera, P. Bongers, M. Henson, *Colloids Surf* **2010**, *361*, 108.
[25] G. Haifeng, L. Wenlong, Z. Xianming, P. Ye, Y. Bao, M. Ying, *Sep. Purif. Technol.* **2019**, *238*, 116397.
[26] M. Manga, H. A. Stone, *J. Fluid Mech.* **1995**, *300*, 63.
[27] X. Zhang, O. A. Basaran, R. M. Wham, *AIChE J.* **1995**, *41*, 1629.
[28] D. Ramkrishna, J. Borwanker, *Chem. Eng. Sci.* **1974**, *29*, 1711.
[29] F. Gelbard, J. H. Seinfeld, *J. Comput. Phys.* **1978**, *28*, 357.
[30] S. Kumar, D. Ramkrishna, *Chem. Eng. Sci.* **1996**, *51*, 1333.
[31] R. McGraw, J. H. Saunders, *Aerosol Sci. Technol.* **1984**, *3*, 367.
[32] J. D. Lister, D. J. Smit, M. J. Hounslow, *AIChE J.* **1995**, *41*, 591.

**How to cite this article:** N. Akbarian Kakhki, M. Shooshtari, M. Karimi, *Can. J. Chem. Eng.* **2024**, 1. https://doi.org/10.1002/cjce.25189